Sulfur-Cycling in Methane-Rich Ecosystems: Uncovering Microbial Processes and Novel Niches

Thesis by
Abigail Green Saxena

In Partial Fulfillment of the Requirements for the degree
of
Doctor of Philosophy

CALIFORNIA INSTITUTE OF TECHNOLOGY
Pasadena, California
2013
(Defended 20 May 2013)

*Chapter 2**

***This chapter, written by Abigail Green Saxena, is currently in review.**

Nitrate-based niche differentiation by distinct sulfate-reducing bacteria involved in the anaerobic oxidation of methane

A. Green-Saxena[1], A. E. Dekas[2,4], N. F. Dalleska[3] and V.J. Orphan[2]

Divisions of [1]Biology and [2]Geological and Planetary Sciences, and [3]Global Environmental Center, California Institute of Technology, 1200 East California Boulevard, Pasadena, CA 91125
[4]Chemical Sciences Division, Lawrence Livermore National Laboratory, P.O. Box 808, L-231, Livermore CA 94551-9900

ABSTRACT

Diverse associations between methanotrophic archaea (ANME) and sulfate-reducing bacterial groups (SRB) often co-occur in marine methane seeps, however the ecophysiology of these different symbiotic associations has not been examined. Here we applied a combination of molecular, geochemical and FISH-NanoSIMS analyses of *in situ* seep sediments and methane-amended sediment incubations from diverse locations (Eel River Basin, Hydrate Ridge and Costa Rican Margin seeps) to investigate the distribution and physiology of a newly identified subgroup of the *Desulfobulbaceae* (seepDBB) found in consortia with ANME-2c archaea, and compared these to the more commonly observed associations between the same ANME partner and the *Desulfobacteraceae* (DSS). Fluorescence *in situ* hybridization (FISH) analyses revealed structured aggregates of seepDBB cells in association with ANME-2 from both environmental samples and laboratory incubations that are distinct in structure relative to co-occurring ANME/*Desulfobacteraceae* consortia (ANME/DSS). ANME/seepDBB aggregates were most abundant in shallow sediment depths below sulfide-oxidizing microbial mats. Depth profiles of ANME/seepDBB aggregate abundance (relative to ANME/DSS aggregate abundance) revealed a positive correlation with elevated porewater nitrate in all seep sites examined. This relationship with nitrate was experimentally confirmed using sediment microcosms, in which the abundance of ANME/seepDBB was greater with the addition of nitrate relative to the unamended control. Additionally, FISH coupled to nanoscale secondary ion mass spectrometry (FISH-NanoSIMS) revealed significantly higher ^{15}N-

nitrate incorporation levels in individual aggregates of ANME/seepDBB relative to ANME/DSS aggregates from the same incubation. These combined results suggest that nitrate is a geochemical effector of ANME/seepDBB aggregate distribution, and may provide a unique niche for these consortia through the utilization of a greater range of nitrogen substrates than the ANME/DSS.

KEY WORDS: niche differentiation, nitrate assimilation, *Desulfobulbaceae*, methane seep, symbiosis

INTRODUCTION

In the decades following the initial implication of sulfate-reducing bacteria in the anaerobic oxidation of methane (AOM; Reeburgh, 1976) significant advances have been made towards understanding the symbiosis responsible for this process. While the availability of the primary respiratory substrates, methane and sulfate, have been shown key to the functioning of this symbiosis (Nauhaus et al., 2005), studies have revealed an unexpected diversity in both the archaeal and bacterial partners capable of AOM (Orphan et al. 2002; Knittel et al. 2005 and 2003; Knittel and Boetius, 2009; Niemann et al., 2006; Pernthaler et al., 2008; Kleindienst et al., 2012; Holler et al 2011).

The archaeal groups ANME-1, -2 and -3 have been found to co-occur at many methane seep sites, but within these sites, specific groups or subgroups often dominate in specific seep habitats (chemosynthetic clam beds or microbial mats) or sediment depth horizons (Nauhaus et al., 2005; Knittel et al., 2005; Krüger et al., 2008; Lloyd et al., 2010; Rossell et al., 2011). Geochemical characterizations of the underlying seep sediment have revealed these distinct chemosynthetic communities are also defined by distinct methane,

sulfate and sulfide gradients (Orphan et al., 2004; Sahling et al., 2002; Torres et al., 2002; Boetius and Suess, 2004). However, the relevant factors selecting for dominant ANME subgroups and their symbiotic sulfate-reducing bacterial partners in these niches have yet to be defined.

The 16S rRNA gene diversity found within and between ANME groups is mirrored by that of their sulfate-reducing bacterial partners (Knittel et al, 2003 and 2005; Schreiber et al, 2010). While seepSRB1a members of the *Desulfobacteraceae* family are the dominant partner of ANME-2 (Schreiber et al., 2010), ANME-3 associates primarily with members of the *Desulfobulbaceae* family (Losekann et al., 2007). However, there appears to be flexibility in partner selection; aggregates of ANME-3 and seepSRB1 cells have been reported (Schreiber et al., 2010), novel ANME-1 consortia have been shown to associate with deltaproteobacteria from the HotSeep-1 cluster (Holler et al., 2011) and ANME-2c (an ANME-2 subgroup) cells were also found in association with those of seepSRB2 (Kleindienst et al., 2012), *Desulfobulbaceae* and other bacteria (Pernthaler et al., 2008). Interestingly, in both of the latter cases these alternative aggregate forms were found coexisting with the dominant consortia type (ANME/DSS), suggesting the different SRB partners may occupy distinct niches.

Cultured members of the *Desulfobacteraceae* and *Desulfobulbaceae* families differ in several key metabolic pathways; *Desulfobulbaceae* contain species capable of sulfur disproportionation as well as using nitrate, metal oxides and sulfur as alternate terminal electron acceptors (Kuever et al., 2005b). While the majority of *Desulfobacteraceae* are capable of complete carbon oxidation, most, if not all, *Desulfobulbaceae* are not (Kuever et al., 2005a and b). Major differences such as these suggest uncultured syntrophic SRB

lineages belonging to these families may also have different ecophysiologies. Although very little is known about which factors lead to differences in syntrophic SRB distribution, it is possible that these same factors are important to the symbiosis as a whole, presenting a unique opportunity to uncover additional environmental regulators of AOM via single cell comparative physiology and distribution of two very distinct syntrophic SRB.

FISH-NanoSIMS (nanoscale secondary ion mass spectrometry) analyses of sediments incubated with stable isotope-labeled substrates allows the simultaneous detection of phylogenetic identity and metabolic activity at single cell resolution. This provides a unique opportunity to investigate potential ecophysiological differences between ANME/DSS and ANME/seepDBB aggregates. Due to the broad substrate range of *Desulfobulbaceae* we used FISH-NanoSIMS to investigate the potential role of nitrogen substrates in defining unique niches for ANME/seepDBB, focusing on nitrate as it is known to be dynamic in methane seep sediments (Bowles and Joye, 2010). Using a combination of molecular, *in situ*, and NanoSIMS analyses of environmental and incubation samples from diverse methane seeps (Eel River Basin, Hydrate Ridge and Costa Rican Margin) we investigated the role of nitrate in ANME/seepDBB (versus ANME/DSS) aggregate distribution and metabolism.

METHODS

Site Selection, Sampling and Processing:

Detailed information for all samples used in this study can also be found in Table S1.

Eel River Basin (AT 15-11) October 2006

Samples from the Northern Ridge of Eel River Basin (40°N 48.6 124°W 36.6; 520 m

water depth), an active methane seep off the coast of Northern California (described in Orphan et al., 2004), were collected by manned submersible Alvin in October of 2006 using push cores. Four, 30 cm long push cores were collected during dive AD4256 along a transect which spanned two habitats defined by distinct chemosynthetic communities residing at the sediment surface in a 'bulls-eye' pattern (governed by sulfide concentration gradients). Microbial mats were present in the center (PC29:mat), surrounded by clam beds (PC17:clam1 and PC23:clam2), which decrease in abundance towards the outer rim of the 'bulls-eye' which has lower methane flux and a low concentration of sulfide (PC20:low methane). Two additional cores, AD4254 PC11 and AD4254 PC14 were collected from a clam bed (40°N 47.2 124°W 35.7) and microbial mat (40°N 47.2 124°W 35.7), respectively, for incubation experiments. Cores were processed shipboard (as described in Pernthaler et al., 2008).

Costa Rica Margin (AT 15-44) February 2009, Hydrate Ridge (AT 15-68) August 2010, Hydrate Ridge (AT 18-10) September 2011

Push core samples were also collected in February 2009 from active methane seeps in the Costa Rica Margin (Mau et al., 2006; Sahling et al., 2008) and Hydrate Ridge (Boetius and Seuss 2004) off the coast of Oregon using manned submersible Alvin and remotely operated vehicle Jason (AT 18-10 only). These push cores were collected through three microbial mats (AD4633 PC2: Hydrate Ridge Mat 1: SE Knoll, 44°N 26.99 125°W 01.69, 625 m water depth, AD4635 PC18: Hydrate Ridge Mat 2: Hydrate Ridge South, 44°N 34.09 125°W 9.14, 775 m water depth; and AD4636 PC19: Hydrate Ridge Mat 3: Hydrate Ridge South, 44°N 34.09 125°W 9.14, 772 m water depth) from Hydrate Ridge and two

microbial mats (AD4510: Jaco Summit, 9°N 10.29 84°W 47.92, 745 m water depth; PC6: Costa Rica Mat 1 and PC1: Costa Rica Mat 2) from Costa Rica Margin. Samples for DNA extractions were also collected from Hydrate Ridge AT 15-68 (AD4629 PC9:Hydrate Ridge South, 44°N 34.1 125°W 9.1, 772 m) and AT18-10 (J2 593 E3 PC47: Hydrate Ridge North, 44°N 40.0 125°W 6.0, 600 m water depth 0-9 cm horizon below microbial mat). All cores for this study were processed shipboard (as described in Pernthaler et al., 2008).

Microcosm experiments

The microcosm experiments used in this study have been previously described by Dekas et al. (2009). Briefly, sediments from Eel River Basin clam bed core AD4254 PC11 (top 12 cm) and microbial mat core AD4254 PC14 (top 15 cm) were mixed approximately 1:1 with filtered seawater sparged with argon. The sediment slurries were amended to 0 or 2 mM ^{15}N-nitrate (PC-11) or 2 mM ^{15}N-ammonium (PC-14) and incubated anaerobically with a headspace of methane (overpressed to 30 PSI) in glass bottles with butyl stoppers at 4-8 ºC. Sediment samples were taken anaerobically via syringe at 3 (nitrate incubations) and 6 months (ammonium incubations). Sediment samples were fixed in 4% formaldehyde for one hour, washed with PBS, then PBS and EtOH (1:1), and then resuspended in EtOH, and stored at -20 C.

DNA Extraction and Clone Library Analysis

DNA was extracted from methane seep sediment collected from Costa Rica (AT15-44 AD4510 PC6: 0-1 cm below a microbial mat), Hydrate Ridge (AT 15-68 AD4629 PC9:Hydrate Ridge South, 44°N 34.1 125°W 9.1, 772 m water depth, 0-3 cm below a

microbial mat; sediment incubated with an initial 500 μm nitrate under 30 psi methane and sampled after 4 months), and from magneto-FISH-captured aggregates (see below for details on magneto-FISH) from Eel River Basin (AT15-11 AD4256 PC29: 3-6 cm horizon below microbial mat) and Hydrate Ridge (AT18-10 J2 593 E3 PC47: Hydrate Ridge North, 44°N 40.0 125°W 6.0, 600 m water depth 0-9 cm horizon below microbial mat) using probes seepDBB653 and ANME_2c_760 (Knittel et al., 2005), respectively. Sediment extractions were conducted using the MoBio Ultraclean soil kit following a previously published protocol (Orphan et al., 2001). DNA extraction from magneto-FISH-captured aggregates was conducted as described in Pernthaler et al. (2008). Following extraction, magneto-FISH DNAs from Eel River Basin were amplified using Multiple Displacement Amplification (MDA performed using REPLI-g Mini Kit from Qiagen, Valencia, CA) prior to PCR amplification.

Bacterial 16S rRNA genes were amplified from Hydrate Ridge, Eel River Basin and Costa Rica Margin samples using bacteria specific forward primer BAC-27F and universal reverse primer U-1492R (Lane, 1991). Thermocycling conditions consisted of an initial 94°C denaturing step for 3 minutes followed by 30 cycles of 94°C for 45 seconds, 54°C for 45 seconds and 72°C for 1 minute 20 seconds, and then a final 72°C elongation step for 7 minutes. Amplification reactions followed published PCR mixtures and conditions (Harrison et al., 2009) with 0.5μl of Hotmaster Taq polymerase (Eppendorf AG, Hamburg, Germany).

Sequencing and Phylogenetic Analysis

The amplified 16S rRNA gene products were cleaned using a Multiscreen HTS

plate (Millipore). The purified amplicons were ligated into pCR 4.0 TOPO TA (Invitrogen Corp., Carlsbad, CA) vectors and used to transform One-Shot TOP10 (Invitrogen Corp., Carlsbad, CA) chemically competent cells according to the manufacturer's instructions. A minimum of 10 clones were cleaned using Multiscreen HTS plates (Millipore, Billerica, MA) and sequenced either in house with a CEQ 8800 capillary sequencer according to the DTCS protocol (Beckman Coulter, Fullerton, CA), at the ASGPB DNA Sequencing Facility of the University of Hawai'i at Manoa or at the Laragen sequencing facility (www.laragen.com).

Sequences were manually edited using Sequencher 4.5 software (Gene Codes, Ann Arbor, MI) and aligned using SILVA online aligner (SINA; http://www.arb-silva.de/aligner) followed by the ARB software package (version 7.12.07org, ARB_EDIT4; Ludwig et al., 2004) into the Silva 108 full-length 16S rRNA gene alignment (http://www.arb-silva.de/). A distance tree of all previously published 16S rRNA genes used for this study, inferred by Neighbor-joining with the Jukes and Cantor model, was used to estimate distances using the ARB database SSURef-108-SILVA-NR (www.arb-silva.de) and the provided bacterial filter. Bootstrap values were obtained in PAUP* 4.0b10 by Neighbor-joining with 1000 bootstraps. Sequences *Acidobacterium capsulatum* (CP0001472), *Terriglobus roseus* (DQ660892), *Acanthopleuribacter pedis* (AB303221) and *Geothrix fermentans* (AB303221) served as outgroups to root the tree. Sequences from this study were added to the existing full-length 16S rRNA tree using the quick add maximum parsimony method. Genbank accession numbers are (KC598077-KC598083).

Probe Design:

An alignment of pure culture and putative *Desulfobulbaceae* 16S rRNA gene sequences retrieved from Eel River Basin by Pernthaler and colleagues (2008) was used to design oligonucleotide probe seepDBB653 (CTTTCCCCTCCGATACTCA). This 19 bp probe contains one mismatch, at position 660, to sequences retrieved in this earlier study that makes the probe less homologous to *Desulfobacteraceae* and more homologous to pure culture *Desulfobulbaceae* reference sequences.

Clone-FISH (Schramm et al., 2002; Wagner et al., 2003) was performed to test seepDBB653 and determine the optimal formamide concentration. Single-use BL21 (DE3) LysS cells (Promega, Madison, WI) were transformed with a Topo TA PCR4.0 vector (Invitrogen, Grand Island, NY) containing a 16S rRNA insert of the original seepDBB sequences extracted from Eel River Basin methane seep by Pernthaler and colleagues (EU622294; Pernthaler et al., 2008). CARD-FISH reactions were performed on resulting cells using a range of formamide concentrations from 10% to 60%. The optimal formamide concentration was 15% to 25%. Subsequent CARD-FISH reactions on environmental samples using probe seepDBB653 yielded an optimal signal at 15% formamide. Likely due to the low formamide concentration, seepDBB653 has a faint cross hybridization with DSS cells, which is clearly discerned from the true signal when dual hybridizations of seepDBB653 and DSS658 probes are conducted. The specificity of seepDBB653 was further tested via a magneto-FISH reaction targeting seepDBB-containing aggregates; all examined bacterial 16S rRNA gene sequences (n = 9 randomly sequenced clones) were within the seepDBB group initially recovered by Pernthaler et al (2008).

Catalyzed Reporter Deposition Fluorescence *in situ* Hybridization (CARD-FISH):

Sediment samples were fixed in 2% formaldehyde for approximately 1.5 hours at room temperature, washed twice with phosphate-buffered saline (PBS; Pernthaler et al., 2008), once with 1:1 PBS: ethanol, resuspended in 100% ethanol and stored at -20°C. For CARD-FISH analyses, 40-75 µl fixed sediment collected from each depth horizon was brought to 1.5 ml in a TE (10 mM Tris-HCl and 1 mM EDTA (pH 9.0)), 0.01 M pyrophosphate solution, heated in a histological microwave oven (Microwave Research and Applications, Carol Stream, IL) for 3 minutes at 60°C, cooled to room temperature and incubated in 0.1% hydrogen peroxide for 10 minutes. The solution was then sonicated on ice for two 5 second bursts with a Vibra Cell sonicating wand (Sonics and Materials, Danbury, CT) at an amplitude setting of 3.0 and overlaid on a Percoll density gradient (Orphan et al., 2002) prior to filtration onto a 3.0 µm pore filter (Millipore, Billerica, MA). Resulting filters were permeabilized in sequential HCl, SDS and lysozyme solutions as described by Pernthaler et al. (2004). Horseradish peroxidase-labeled probes (Biomers, Ulm, Germany) targeting seep *Desulfobulbaceae* (seepDBB653, 15% formamide; this study) and either *Desulfobacteraceae* (DSS_658, targets *Desulfosarcina* spp./*Desulfococcus* spp./*Desulfofrigus* spp. and *Desulfofaba* spp; Manz et al., 1998) or anaerobic methane-oxidizing archaeal clade ANME-2 (Eel_MS_932; Boetius et al., 2000) were then used in a dual-hybridization CARD-FISH reaction (Pernthaler et al., 2008). The first hybridization reaction was conducted in a histological microwave oven for 30 minutes at 46°C, followed by an amplification reaction using fluorescein-labeled tyramides. The second hybridization reaction was carried out in a hybridization oven for 2.5 hours at 46°C followed by an amplification reaction using Alexa Fluor 546-labeled tyramides. Samples were then counter

stained with 4',6' -diamidino-2-phenylindole (DAPI). Micrograph images were taken with a Deltavision RT microscope system (Applied Precision, Issaquah, WA).

Magneto-FISH:

Magneto-FISH was performed on 75 µl of fixed sediment, with probes Eel_MS_932 (Boetius et al., 2000) and seepDBB653, as described in (Pernthaler et al., 2008) with the following modifications. During the amplification reactions, 0.1% blocking reagent was used instead of BSA. Following the CARD-FISH reaction, monoclonal mouse anti-fluorescein-antibodies (Molecular Probes) were applied directly to the sediment (approximately 1 µg/10^6 cells), incubated for 10 minutes on ice, and washed via two centrifugation steps at 300 x g for 8 minutes with re-suspension in PBS (containing 0.1% BSA; pH 7.4) in 1.5 ml tubes. Sediment was then incubated with pan-mouse paramagnetic beads (5 µm diameter; approximately 25 µl/10^7 cells) (Dynal, AS, Norway) at 4°C, rotating, for one hour. Tubes of sediment were then washed 15 times by placing near a magnet (Dynal MPC-E) for 2 minutes, removing supernatant and re-suspending in PBS (containing 0.1% BSA; pH 7.4), with a final re-suspension in TE prior to DNA extraction.

Morphological Data:

Morphological data were collected from ANME/seepDBB aggregates (using probes seepDBB653 probe and Eel_MS_932) in sediment samples from four push cores collected along a transect within an Eel River Basin methane seep. A total of 86 positively hybridized aggregates were imaged and characterized as one of the following morphotypes: shell, partial shell, clumped or mixed (Figure S2).

Morphological data were also collected from ANME/seepDBB and ANME/DSS aggregates (using probes seepDBB653 probe and DSS_658, respectively) in Eel River Basin sediment incubated with 2 mM ^{15}N-nitrate or ^{15}N-ammonium and sampled at 4 or 6 months, respectively. A total of 84 aggregates were imaged, characterized as one of the four morphotypes (shell, partial shell, clumped or mixed).

Aggregate counts:

Nitrate depth profiles (details below) were used to select low (< 50 μM nitrate) and high (> 50 μM nitrate) nitrate cores to examine via CARD-FISH. Depth profiles of relative DAPI/seepDBB (versus DAPI/DSS) aggregate abundance were generated from these push cores, which were collected through three microbial mats (AD4633 PC2: Hydrate Ridge Mat 1, AD4635 PC18: Hydrate Ridge Mat 2 and AD4636 PC19: Hydrate Ridge Mat 3) from Hydrate Ridge and two microbial mats (AD4510 PC6: Costa Rica Mat 1 and AD4510 PC1: Costa Rica Mat 2) from Costa Rica Margin. Samples for aggregate counts were obtained from 1 cm (Hydrate Ridge Mat 2 and Costa Rica Mat 1) or 3 cm (Hydrate Ridge Mats 1 and 3 and Costa Rica Mat 2) core slices and hybridized with probes seepDBB653 and DSS_658. DAPI/seepDBB and DAPI/DSS aggregates were counted from a total of 50 aggregate-containing fields per sample. Relative numbers of DAPI/seepDBB aggregates are expressed as percent DAPI/seepDBB of total DAPI/SRB aggregates.

Samples for Eel River Basin aggregate counts were obtained from 3 cm core slices and hybridized with probes seepDBB653 and Eel_MS_932. A total of 100 ANME-containing aggregates were counted per sample. Relative numbers of ANME/seepDBB aggregates are expressed as percent ANME/seepDBB of total ANME-containing

aggregates. Total aggregate counts were also done via epifluorescent microscopy after staining the sediment with DAPI. Briefly, 0.1 to 0.5 µl of fixed and washed sample, diluted in PBS, was filtered onto 0.22 µm pore filters (Millipore, Billerica, MA) and enumerated according to Turley (1993).

Samples for incubation aggregate counts came from a previously described push core collected through a clam bed in Eel River Basin (PC11) and incubated with and with out 2 mM nitrate under a methane headspace as described in Deskas et al., (2009). After performing a Percoll density separation as describe above, samples were hybridized with probes seepDBB653 and DSS_658 (Manz et al., 1998). DAPI/seepDBB and DAPI/DSS aggregates were counted from a total of fifty aggregate-containing fields per sample. Due to sample limitation, counts were made from 3 replicate methane-only incubations and from 3 filter wedges from one nitrate-amended incubation. Relative numbers of DAPI/seepDBB aggregates are expressed as percent DAPI/seepDBB of total DAPI/SRB aggregates.

Geochemical:

Geochemical depth profiles (at 3 cm resolution) of methane, sulfate and sulfide concentrations were generated from push cores collected at Eel River Basin. Methane and sulfate were measured via ion and gas chromatography as described by Orphan and colleagues (2004). Sulfide was measured using the Cline Assay (Cline, 1969) as described by Dekas and colleagues (2009).

Nitrate and nitrate concentrations for Costa Rica Margin samples were analyzed with an

Antek chemiluminescence detector at the University of Georgia, Athens, and reported in (Dekas et al., submitted).

Nitrate concentrations for Hydrate Ridge samples were measured as follows. Pushcore pore-water squeezed from sediments immediately after collection was filtered via a 0.2 μm filter and frozen at -20˚C until analysis. Parallel ion chromatography systems operated simultaneously (Dionex DX-500, Environmental Analysis Center, Caltech) were used to measure ammonium, nitrate, nitrite and sulfate in the porewater samples. A single autosampler loaded both systems' sample loops serially. The 10 μl sample loop on the anion IC system was loaded first, followed by a 5 μl sample loop on the cation IC system. Temperatures of the columns and detectors were not controlled. Measurements of cationic species is not presented in this work so is not discussed further.

Nitrite, nitrate and sulfate were resolved from other anionic components in the sample using a Dionex AS-19 separator (4x250 mm) column protected by an AG-19 guard (*4x50 mm). A hydroxide gradient was produced using a potassium hydroxide eluent generator cartridge and pumped at 1 mL per minute. The gradient began with a 10 mM hold for 5 minutes, increased linearly to 48.5 mM at 27 minutes and finally to 50 mM at 41 minutes. 10 minutes were allowed between analyses to return the column to initial conditions. Nitrite and nitrate were determined for UV absorption at 214 nm using a Dionex AD25 Absorbance detector downstream from the conductivity detection system. Suppressed conductivity detection using a Dionex ASRS-300 4 mm suppressor operated in eluent recycle mode with an applied current of 100 mA was applied to detect all other anions, including redundant measurement of nitrite and nitrate. A carbonate removal

device (Dionex CRD 200 4 mm) was installed between the suppressor eluent out and the conductivity detector eluent in ports.

Standard curves were generated for each species. For nitrate, nitrite, and sulfate, standard measurements were fitted to a linear curve. Standard ranges were 10 μM to 2 mM (nitrate, nitrite) and 500 μM to 32 mM (sulfate). Standard deviation of repeated injections of a standard (250 μM nitrate and nitrite, 8000 μM sulfate) throughout the analysis were 4.2 μM (nitrate), 5.8 μM (nitrate) and 113 μM (sulfate).

Fluorescence *in situ* Hybridization Nanoscale Secondary Ion Mass Spectrometry (FISH-NanoSIMS):

Thirteen ANME/SRB aggregates (7 ANME/seepDBB and 6 ANME/DSS) were examined from an ammonium-amended incubation (approximately 2 mM ^{15}N-ammonium, sampled at 6 months) inoculated with methane seep sediment slurries from a push core collected through a microbial mat in Eel River Basin (PC-14; Dekas et al, 2009). Fourteen ANME/SRB aggregates (6 ANME/seepDBB and 8 ANME/DSS) were examined from a nitrate-amended incubation (2 mM ^{15}N-nitrate, sampled at 3 months) inoculated with methane seep sediment slurries from a push core collected through a clam bed in Eel River Basin (PC-11; Dekas et al., 2009).

All samples were deposited onto 1” diameter round microprobe slide (Lakeside city, IL) and hybridized with HRP-labeled probes seepDBB653 and DSS_658; DAPI/seepDBB and DAPI/DSS aggregates were then mapped for nanoSIMS analysis (Orphan et al., 2002; Dekas and Orphan, 2011). Clostridia spores (with known δ^{13}C and δ^{15}N) were spotted onto a blank section of the glass and used as standards during the analysis. Samples were then

gold-coated and analyzed using a CAMECA NanoSIMS 50L housed at Caltech, using a mass resolving power approximately 5,000. A primary Cs^+ ion beam (4.3 to 22 pA) was used to raster over target cells, with a raster size ranging from 8 to 25 μm. Secondary ion images were collected at 256 x 256 pixel resolution with a dwell time of 14,000 ct/pixel over a period of 4 to 20 hours, resulting in 7 to 97 cycles, depending on target size. This range of ion beam current was used to maximize counts with no offset in ^{15}N observed in standards run before and after the analysis. Clostridia spores were measured periodically as a standard to ensure there were no matrix effects throughout the analysis in isotope mode using the same range in ion beam current. Several masses were collected in parallel including: $^{12}C^{14}N^-$, and $^{12}C^{15}N^-$ using electron multiplier detectors. Resulting ion images were processed using the L'Image software (developed by L. Nittler, Carnegie Institution of Washington, Washington D.C.). The reported isotope ratio for each aggregate was extracted from the image by identifying a region of interest – the aggregate – within each image. The aggregate edge was automatically defined in L'image by setting a lower threshold of 35% of the maximum value of $^{12}C^{15}N/^{12}C^{14}N$ counts within a given cycle. The ratio from the cycle with the highest $^{12}C^{15}N/^{12}C^{14}N$ was then collected from each aggregate. The $^{12}C^{15}N/^{12}C^{14}N$ ratio is hereafter referred to as the $^{15}N/^{14}N$ ratio.

RESULTS

Phylogenetic characterization of *Desulfobulbaceae* from multiple seeps

Bacterial 16S rRNA gene sequences distantly related to cultured *Desulfobulbaceae* sequences were recovered from methane seep sediment collected from Costa Rica and Hydrate Ridge. These sequences formed a well-supported clade putatively within the

Desulfobulbaceae family, along with seepDBB sequences previously retrieved from magneto-FISH enriched ANME-2c aggregates from Eel River Basin (Pernthaler et al., 2008), and distinct from the ANME-3 partners and previously described seepSRB3 and seepSRB4 clades (Knittel et al., 2005); (Figure 1). Initial Eel River Basin sequence data from this clade were used to design an oligonucleotide probe for CARD-FISH analyses of ANME/seepDBB consortia in situ.

Aggregate characterization

Environmental data

A total of 86 positively hybridized ANME/seepDBB aggregates from Eel River Basin samples were characterized by aggregate morphology, with the majority of *Desulfobulbaceae* aggregates consisting of partial shell (37%) followed by whole shells and clumped aggregates (24% and 27%, respectively); mixed aggregates represented 12% (Figure 2b, S3). The majority (75%) of examined aggregates were 2-6 μm in diameter, with smaller percentages forming aggregates greater than 6 μm.

Incubation data

Similar to the *in situ* observations, the dominant ANME/seepDBB morphology in the nitrate incubation was also partial shell (69%), followed by mixed (19%) and clumped aggregates (13%; Figure 2a). The ANME/seepDBB aggregates in the ammonium incubation were dominated by clumped morphology (44%), followed by partial shell (34%), whole shell (16%) then mixed (19%; Figure 2a). The average ANME/seepDBB aggregate diameter was 6.6 μm in the nitrate incubation and 4.5 μm in the ammonium

incubation.

The dominant ANME/DSS morphology in the nitrate incubation was whole shell (50%), followed by equal proportions of mixed and partial shells (25%), with no clumped aggregates detected (Figure 2c). The ammonium incubation in contrast, was dominated by mixed ANME/DSS morphology (45%), followed by clumped (35%), partial shell (15%) and whole shell (5%).

Geochemistry and ANME/seepDBB distribution in diverse methane seep environments

Eel River Basin (AT 15-11)

The seepDBB653 probe along with Eel_MS_932 (targeting ANME cells, Boetius et al., 2000) was initially used to calculate abundance of aggregates associated with the three main seep habitats (clam, mat, low-methane flux periphery) and with increasing sediment depth. Four cores were selected along a transect (*mat, clam1, clam2* and *low methane*) containing one central mat, two flanking clam beds and the surrounding sediment.

The relative ANME/seepDBB aggregate abundance decreased with depth in 3 of 4 cores (mat, clam2 and low-methane flux site; Figure S1). The geochemical profiles of clam1 indicate relatively low levels of sulfate depletion compared to clam2 and mat, perhaps resulting from lower methane flux along the periphery of the clam bed. The apparent correlation between relative ANME/seepDBB aggregate abundance and depth seen in mat, clam2 and low methane did not appear to be related to sulfate, sulfide or methane concentrations.

Costa Rican Margin (AT 15-44) and Hydrate Ridge (AT 15-68)

Porewater nitrate concentration profiles were used to select cores containing greater than 50 μM nitrate for further analysis. Nitrate profiles from Costa Rica Margin cores are previously described in Dekas et al. (in review). Cores collected through microbial mats had the highest levels of porewater nitrate of the habitats examined, with the greatest concentrations associated with sediments just below microbial mats, similar to previous reports (Bowles and Joye, 2010). The cores examined in this study contained nitrate ranging from 97 to 1227 μM in the shallowest depth horizon (0-3 cmbsf in Hydrate Ridge Mat1, 0-1 cmbsf in Costa Rica Mat and Hydrate Ridge Mat2) that decreased below the detection limit in the deeper depth horizons (> 7 cmbsf; Figure 3). Depth profiles of relative DAPI/seepDBB (versus DAPI/DSS) aggregate abundance positively correlated with those of nitrate in the resulting cores in both Hydrate Ridge and the Costa Rican Margin (n = 3 cores). Low-nitrate (< 50 μM nitrate) cores were also examined (n = 2 cores), revealing consistently low (DAPI/seepDBB aggregates < 10% of total aggregates) relative DAPI/seepDBB (versus DAPI/DSS) aggregate abundance.

Microcosm Analyses via FISH-NanoSIMS

CARD-FISH analyses using probes seepDBB653 and DSS658 were employed on previously prepared methane-amended incubations of seep sediment from the Eel River Basin supplemented with 2 mM nitrate, 2 mM ammonium or no amendment (Dekas et al. 2009). The relative abundance of ANME/seepDBB aggregates (represented as a fraction of total DAPI/SRB aggregates) at 3 months was greater in the nitrate-amended incubation (0.146; Std Err Mean = 0.027) than a non-amended control (0.087; Std Err Mean = 0.010).

A total of fourteen ANME/SRB aggregates (6 ANME/seepDBB and 8 ANME/DSS) were examined via FISH-NanoSIMS from the same nitrate-amended microcosm at 3 months. Significantly higher maximum ^{15}N incorporation levels were observed in ANME/seepDBB (versus ANME/DSS) aggregates where $^{15}N/^{14}N$ ratios ranged from 0.07 to 0.19 in ANME/seepDBB aggregates and from 0.01 to 0.09 in ANME/DSS aggregates (Figure 4; nonparametric Wilcoxon Pval = 0.024). Overall levels of ^{15}N enrichment were likely lower in nitrate-amended (relative to ammonium-amended) incubations due to differences in sediment source, sampling times and ability of microorganisms to assimilate the two nitrogen sources, as previously observed in Dekas et al. (2009). Isotope imaging showed that several of the aggregates (n = 6) from the ^{15}N-nitrate-amended incubation exhibited highest ^{15}N enrichment in the region corresponding to SRB cells (Figure 5).

To compare relative uptake of ^{15}N-ammonium, a total of thirteen ANME/SRB aggregates (7 ANME/seepDBB and 6 ANME/DSS) were examined via FISH-NanoSIMS from the ammonium-amended microcosm (sampled at 6 months). There was no significant difference in maximum ^{15}N incorporation levels between ANME/seepDBB and ANME/DSS aggregates (Figure 4; nonparametric Wilcoxon Pval = 0.175). $^{15}N/^{14}N$ ratios for ranged from 0.81 to 1.39 in ANME/seepDBB aggregates and from 0.60 to 2.07 in ANME/DSS aggregates. At 6 months the level of ^{15}N enrichment in ammonium-amended incubations was too high ($^{15}N/^{14}N$ ratios ranged from 0.60 to 2.07) to distinguish higher incorporation levels in SRB regions versus ANME regions of the aggregate.

DISCUSSION

Molecular tools such as 16S rRNA gene surveys have advanced environmental microbiology towards an understanding of the diversity of communities residing in an ecosystem (Lane, 1991; Pace et al., 1985). This has afforded knowledge of community composition and relative abundance of phylotypes that has become increasingly more accurate as our sequence technologies progress towards the ability to deeply sample the 16S rRNA diversity in an environment (Prosser et al., 2012). This increasing level of detail in our knowledge of community diversity opens up more questions, such as how microorganisms in such a complex community not only relate to each other but also to the environment they inhabit. Stable isotope probing allows the simultaneous detection of identity and metabolic capability (Dumont and Murrell, 2005). Using methods affording a finer scale of spatial resolution, such as FISH-SIMS, HISH-SIMS, and microfluidic digital PCR (Orphan et al., 2001; Musat et al., 2008; Ottesen et al., 2006), we can begin to tease out the function of specific members of a community, and particularly with isotopic approaches, we can understand metabolic processes connecting these organisms to one another and their environment.

Characterization of seepDBB partner

Compared to the ANME, very little is known about the potential physiologies or habitat preferences of the various groups of SRB involved in AOM (Knittel and Boetius, 2009). Though a recent study reports seepSRB1a members of the *Desulfobacteraceae* family are the dominant partner of ANME-2 (Schreiber et al., 2010), other SRB and unknown bacterial partners have been documented for ANME-2 (Orphan et al., 2002; Knittel et al., 2005; Kleindienst et al., 2012; Pernthaler et al., 2008; Schreiber et al., 2010). Using an

immuno-magnetic cell capture technique (magneto-FISH) to enrich for ANME-2c aggregates, Pernthaler and colleagues (2008) reported the detection of ANME/*Desulfobulbaceae* co-existing with ANME/DSS aggregates and phylogenetically distinct from the *Desulfobulbaceae* group previously described in association with ANME-3 (Niemann et al., 2006; Losekann et al., 2007; Figure 1). Here we studied the distribution and ecophysiology of co-occurring SRB/ANME consortia, as well as expanded the known distribution of ANME-associated *Desulfobulbaceae* (seepDBB) cells.

SeepDBB was first described from a single sample collected from a seep site at Eel River Basin (Pernthaler et al., 2008); in the present study CARD-FISH analyses were used to better characterize the depth and habitat distribution of the ANME/seepDBB consortia. We examined push cores from a transect spanning three habitats (a sulfur-oxidizing microbial mat, a Calyptogena clam bed and the peripheral sediments with lower methane flux) within this methane seep. Incubations of Eel River Basin sediment amended with either 2 mM nitrate or ammonium were also examined. The majority of ANME/seepDBB aggregates from both environmental and incubation data sets were 2-7 μm in diameter and had either a partial shell or clumped morphology (Figure 2a and 2b). Interestingly, while these morphotypes were also observed in ANME/DSS aggregates, the dominant morphology was either whole shell or mixed (Figure 2c), suggesting different dynamics may exist between the partners comprising ANME/seepDBB versus ANME/DSS consortia.

Percoll density gradients were used in this study to concentrate aggregates from fixed sediments prior to CARD-FISH analyses and are likely necessary for ANME/seepDBB detection in many methane seep habitats due to their lower abundance, which may explain the lack of their detection in previous studies (eg, Schreiber et al., 2010). When the relative

number of the ANME/seepDBB aggregates are low, fluorescence *in situ* hybridization in sediment samples often requires significant dilution to avoid masking of cells by particles. Use of these density based or magnetic enrichment methods (magneto-FISH; Pernthaler et al., 2008) enable the processing of a greater amount of sediment, increasing the potential for detecting rarer phylotypes.

While ANME/seepDBB aggregates were found in all Eel River Basin habitats examined, as well as below microbial mat habitats in HR and CR methane seeps, they were always found as a lower proportion of total ANME/SRB aggregates relative to ANME/DSS (Figures S1 and 3). Despite the relative difference in abundance, the consistent coexistence of two types of ANME/SRB aggregates could result from niche partitioning, which has been demonstrated in cultured species of SRB within the same class (Dar et al., 2007). ANME-associated DSS and seepDBB belong to distinct families (*Desulfobacteraceae* and *Desulbulbaceae*, respectively) whose cultured representatives differ in several key metabolic pathways (Kuever et al., 2005a and b). With the possible exception of *Desulfofustis*, no genera in the *Desulfobulbaceae* family are capable of completely oxidizing carbon substrates, whereas most genera of *Desulfobacteraceae* family can (Kuever et al., 2005a and b). The *Desulfobulbaceae* are also distinct for harboring species capable of sulfur disproportionation as well as respiring metal oxides, nitrate and sulfur as alternate terminal electron acceptors (Kuever et al., 2005b). Indeed, Milucka and colleagues (2012) recently proposed ANME-2 to be capable of both the anaerobic oxidation of methane and reduction of sulfate to disulfide (or other S^0 compounds), which is scavenged by the DSS and disproportionated to sulfide and sulfate. In this model, multiple SRB can serve as disulfide scavengers, including *Desulfobulbaceae*, but it remains

unclear why multiple syntrophic SRB lineages co-exist. Major differences between cultured members of the *Desulfobacteraceae* and *Desulfobulbaceae* families suggest these syntrophic SRB lineages may also have distinct ecophysiologies, which we first explored by comparing their distribution in diverse methane seeps to the geochemical gradients in these habitats.

Geochemical profiles and ANME/seepDBB distribution in diverse methane seep environments

Investigated cores from Eel River Basin were collected along a transect spanning multiple seep habitats (Figure S1). ANME/seepDBB aggregates were typically most abundant in the shallower depth horizons of the Eel River Basin transect, with the greatest relative proportions documented below a sulfur-oxidizing microbial mat (Figure S1). Available depth profiles of methane, sulfate and sulfide did not appear to explain this distribution. A review of published 16S rRNA and FISH-based studies reporting the presence of *Desulfobulbaceae* in methane seep sediment also revealed an increase in seepDBB-affiliated cells and sequences in shallow horizons beneath sulfur-oxidizing microbial mats (Orphan et al,. 2001; Knittel et al., 2003; Niemann et al., 2006; Losekann et al., 2007, Pernthaler et al., 2008). While geochemical porewater profiles for methane, sulfate and sulfide in the 0 – 10 cm sediment horizons are highly variable between methane seep sites (Knittel and Boetius, 2009; Lloyd et al., 2010; Bowles et al., 2011; Niemann et al., 2006; Valentine and Reeburgh, 2000; Linke et al., 2005), nitrate levels from methane seeps are typically highest just below microbial mats (Linke et al., 2005; Bowles et al., 2010; Priesler et al., 2007; Lichtschlag et al., 2010). Given the documented nitrate usage by

cultured members of the *Desulfobulbaceae* and their high relative abundance in near seafloor sediments beneath microbial mats, we hypothesized nitrate to be one potential geochemical effector of ANME/seepDBB aggregate distribution, and focused subsequent studies on sediment cores varying in nitrate concentration.

Environmental trends in seepDBB abundance from Costa Rican margin and Hydrate Ridge methane seep sites suggested a potential relationship with nitrate. Highest proportions of ANME/seepDBB (> 35% of all ANME/SRB aggregates) were seen in the shallow horizons of the Costa Rica Margin core where two peaks of increased ANME/seepDBB aggregates were observed at different depths. Interestingly this was the only core that had two peaks of increased nitrate concentrations, which roughly correspond to the increase in ANME/seepDBB aggregates (Figure 3d). To understand the relationship between seepDBB cells and nitrate, we next studied the effects of nitrate-amendment on the anabolic activity of ANME/seepDBB and ANME/DSS aggregates in microcosms of methane seep sediment.

Nitrate utilization by ANME/seepDBB aggregates

Methane seep sediment previously collected from Eel River Basin and amended with 2 mM ^{15}N-labeled nitrate or ammonium (under methane headspace; Dekas et al., 2009) was used in the current study for CARD-FISH and NanoSIMS analyses. Active sulfide production was previously measured from both incubations (Dekas et al., 2009). After three months the relative abundance of ANME/seepDBB (represented as a percent of total DAPI/SRB aggregates) was greater in the nitrate-amended incubation 0.146) than the non-amended control (0.087). The reported doubling time of ANME/SRB aggregates has

been estimated between 3 to 7 months (Orphan et al., 2009; Nauhaus et al., 2007), and the increase in seepDBB documented here may result both from the growth/division of new ANME/SRB aggregates as well as from an increase in the size of smaller aggregates less than < 3 μm in diameter into sizes large enough to be retained on the 3 μm pore size filter used for density gradient separation prior to CARD-FISH (ANME/seepDBB from this incubation had an average diameter of 6.6 μm).

Higher maximum ^{15}N incorporation levels were observed in ANME/seepDBB aggregates versus ANME/DSS aggregates from the ^{15}N-nitrate incubation (Figure 4a), while there was no significant difference in maximum ^{15}N incorporation levels between ANME/seepDBB and ANME/DSS aggregates from the ^{15}N-ammonium incubation (Figure 4b). These data suggest similar assimilation rates for ANME/seepDBB and ANME/DSS in the presence of ammonium, and control for the possible artifact of overall higher growth rates in ANME/seepDBB (versus ANME/DSS) aggregates leading to increased incorporation of any labeled nutrient. Previous FISH-SIMS studies using ^{15}N-labeled ammonium- and N_2-amended sediment incubations showed the greatest ^{15}N assimilation by the ANME archaea (Orphan et al., 2009; Dekas et al., 2009). In contrast, several ANME/SRB aggregates analyzed from the labeled nitrate incubation showed clear ^{15}N enrichment in the region associated with SRB cells (Figure 5), suggesting that the SRB partner may be responsible for the majority of the nitrogen incorporation from nitrate in these aggregates.

Although ANME/seepDBB aggregates were consistently less abundant than ANME/DSS, their role in nitrate processing may afford them a more prominent role in marine methane seep ecosystems than their numbers suggest. Keystone species are not necessarily the most

abundant members of the community, for example, FISH-NanoSIMS analysis by Musat and colleagues showed that *Chromatium okenii*, representing approximately 0.3% of total microbial cell numbers, was responsible for over 40% of total ammonium uptake and 70% of total carbon fixation in oligotrophic, meromictic Lake Cadagno (Musat et al., 2008). While our results indicate that ANME/seepDBB aggregates have a greater capability (or preference) than ANME/DSS for using nitrate, it is currently unclear if ANME/seepDBB aggregates are using nitrate for anabolism, respiratory energy, or both. Studies of nitrate-reducing SRB in pure culture have documented the dissimilatory reduction of nitrate to ammonium (DNRA), which can then be incorporated into biomass (Rabus et al., 2006). Thus both dissimilatory and assimilatory pathways for nitrate reduction in these SRB could lead to incorporation of nitrogen sourced from the ^{15}N nitrate into biomass.

The co-existence of physiologically related species may be explained by niche partitioning (Gause, 1934). Complex environments, such as those encountered in seep sediments, are defined by steep chemical gradients, which can lead to distinct microniches, and, in turn, can result in diversification of species harbored in these habitats (Gray et al., 1999; Torsvik et al., 2002). The observed preference for nitrate by ANME/seepDBB versus ANME/DSS aggregates may be one such mechanism by which two apparently functionally redundant consortia can coexist via partitioning the environment into niches defined by nitrogen source.

CONCLUSIONS

Very little is known about factors influencing the distribution and fitness of distinct sulfate-reducing bacteria partnered with methanotrophic ANME archaea. Poorly

constrained ecological and physico-chemical factors are almost certainly important to the AOM symbiosis as a whole, and present a unique opportunity to uncover additional environmental regulators of sulfate-dependent methane oxidation. Most studies to date have focused on the dynamics of carbon and sulfur metabolism by the AOM symbiosis. Here we demonstrate a role for nitrate as a geochemical effector influencing the distribution of *Desulfobulbaceae*-ANME consortia within methane seeps. While bulk geochemical and molecular analyses provide information on community level diversity and activity, complementary single cell techniques, like the FISH-NanoSIMS method used in this study, provide direct information on the metabolic function of phylogenetically identified microorganisms *in situ* and allow for the assessment of ecophysiological differences among co-existing microbial species.

ACKNOWLEDGEMENTS

We would like to acknowledge Grayson Chadwick for his help with image analysis, Elizabeth Trembath-Reichert for contributing clone sequences, Ankur Saxena for figure design, Yunbin Guan for his assistance with NanoSIMS, Tsege Embaye for methane and sulfate measurements from AT 15-11 and the science party of cruises AT 15–11, AT 15-44, AT 15-68 and AT 18-10 and pilots of the D.S.R.V. Alvin and R.O.V. Jason for their assistance with various aspects of this work. Funding for this work was provided by the Department of Energy Division of Biological Research (DE-SC0004949; to V.J.O.), and a National Science Foundation Graduate Research Fellowship (to A.G.-S.). Samples were collected with funding from the National Science Foundation (BIO-OCE #0825791; to V.J.O.).

REFERENCES

Boetius A, Ravenschlag K, Schubert CJ, Rickert D, Widdel F, Gieseke A, et al. (2000) A marine microbial consortium apparently mediating anaerobic oxidation of methane. Nature 407: 623-626.

Boetius A & Suess E. (2004) Hydrate Ridge: a natural laboratory for the study of microbial life fueled by methane from near-surface gas hydrates. Chemical Geology 205: 291-310.

Bowles M & Joye S. (2010) High rates of denitrification and nitrate removal in cold seep sediments. The ISME journal 5: 565-567.

Bowles MW, Samarkin VA, Bowles KM & Joye SB. (2011) Weak coupling between sulfate reduction and the anaerobic oxidation of methane in methane-rich seafloor sediments during ex situ incubation. Geochimica et Cosmochimica Acta 75: 500-519.

Cline JD. (1969) Spectrophotometric determination of hydrogen sulfide in natural waters. Limnology and Oceanography 454-458.

Dar S, Stams A, Kuenen J & Muyzer G. (2007) Co-existence of physiologically similar sulfate-reducing bacteria in a full-scale sulfidogenic bioreactor fed with a single organic electron donor. Applied Microbiology and Biotechnology 75: 1463-1472.

Dekas AD, Poretsky RS & Orphan VJ. (2009) Deep-sea archaea fix and share nitrogen in methane-consuming microbial consortia. Science 326: 422-426.

Dekas AE & Orphan VJ. (2011) Identification of diazotrophic microorganisms in marine sediment via fluorescence *in situ* hybridization coupled to nanoscale secondary ion mass spectrometry (FISH-NanoSIMS). Methods Enzymol 486: 281-305.

Dekas, AE, Chadwick, GL, Bowles, MW, Joye, SB and Orphan, VJ. (in review) Spatial distribution of nitrogen fixation in methane seep sediment and the role of the ANME Archaea.

Dumont, MG, & Murrell, JC. (2005). Stable isotope probing—linking microbial identity to function. Nature Reviews Microbiology, 3(6), 499-504.

Gause G. (1934) The struggle for existence. Williams and Wilkins, Baltimore.

Gray N, Howarth R, Rowan A, Pickup R, Jones JG & Head I. (1999) Natural communities of Achromatium oxaliferum comprise genetically, morphologically, and ecologically distinct subpopulations. Applied and Environmental Microbiology 65: 5089-5099.

Harrison BK, Zhang H, Berelson W & Orphan VJ. (2009) Variations in archaeal and bacterial diversity associated with the sulfate-methane transition zone in continental margin sediments (Santa Barbara Basin, California). Applied and Environmental Microbiology 75: 1487-1499.

Holler T, Widdel F, Knittel K, Amann R, Kellermann MY, Hinrichs K-W, et al. (2011) Thermophilic anaerobic oxidation of methane by marine microbial consortia. The ISME journal 5: 1946-1956.

Kleindienst S, Ramette A, Amann R & Knittel K. (2012) Distribution and *in situ* abundance of sulfate‚Äêreducing bacteria in diverse marine hydrocarbon seep sediments. Environmental Microbiology.

Knittel K & Boetius A. (2009) Anaerobic Oxidation of Methane: Progress with an unknown process. Annu. Rev. Microbiol. 63: 311-334.

Knittel K, Boetius A, Lemke A, Eilers H, Lochte K, Pfannkuche O, et al. (2003) Activity, Distribution, and Diversity of Sulfate Reducers and Other Bacteria in Sediments above Gas Hydrate (Cascadia Margin, Oregon). Geomicrobiology Journal 20: 269 - 294.

Knittel K, Losekann T, Boetius A, Kort R & Amann R. (2005) Diversity and distribution of methanotrophic archaea at cold seeps. Applied and Environmental Microbiology 71: 467-479.

Krüger M, Blumenberg M, Kasten S, Wieland A, Känel L, Klock J-H, et al. (2008) A novel, multi-layered methanotrophic microbial mat system growing on the sediment of the Black Sea. Environmental Microbiology 10: 1934-1947.

Kuever J, Rainey F & Widdel F. (2005a) Family I. Desulfobacteraceae fam. nov. Bergey's Manual® of Systematic Bacteriology. (Brenner DJ, Krieg NR, Garrity GM, et al., eds.), pp. 960-962. Springer US.

Kuever J, Rainey F & Widdel F. (2005b) Family II. Desulfobulbaceae fam. nov. Bergey's Manual® of Systematic Bacteriology. (Brenner DJ, Krieg NR, Garrity GM, et al., eds.), pp. 988-992. Springer US.

Lane D. (1991) 16S/23S rRNA sequencing. Nucleic acid techniques in bacterial systematics.

Lichtschlag A, Felden J, Brüchert V, Boetius A & De Beer D. (2010) Geochemical processes and chemosynthetic primary production in different thiotrophic mats of the Håkon Mosby Mud Volcano (Barents Sea). Limnology and Oceanography 55.

Linke P, Wallmann K, Suess E, Hensen C & Rehder G. (2005) *In situ* benthic fluxes from an intermittently active mud volcano at the Costa Rica convergent margin. Earth and Planetary Science Letters 235: 79-95.

Lloyd KG, Albert DB, Biddle JF, Chanton JP, Pizarro O & Teske A. (2010) Spatial Structure and Activity of Sedimentary Microbial Communities Underlying a Beggiatoa spp. Mat in a Gulf of Mexico Hydrocarbon Seep. PLoS ONE 5: e8738.

Losekann T, Knittel K, Nadalig T, Fuchs B, Niemann H, Boetius A & Amann R. (2007) Diversity and abundance of aerobic and anaerobic methane oxidizers at the Haakon Mosby mud volcano, Barents Sea. Applied and Environmental Microbiology 73: 3348-3362.

Ludwig W, Strunk O, Westram R, Richter L, Meier H, Buchner A, et al. (2004). ARB: a software environment for sequence data. Nucleic acids research, 32(4), 1363-1371.

Manz W, Eisenbrecher M, Neu TR & Szewzyk U. (1998) Abundance and spatial organization of Gram-negative sulfate-reducing bacteria in activated sludge investigated by *in situ* probing with specific 16S rRNA targeted oligonucleotides. Fems Microbiology Ecology 25: 43-61.

Mau S, Sahling H, Rehder G, Suess E, Linke P & Soeding E. (2006) Estimates of methane output from mud extrusions at the erosive convergent margin off Costa Rica. Marine Geology 225: 129-144.

Milucka J, Ferdelman TG, Polerecky L, Franzke D, Wegener G, Schmid M, et al. (2012) Zero-valent sulphur is a key intermediate in marine methane oxidation. Nature 491: 541-546.

Musat N, Halm H, Winterholler B, Hoppe P, Peduzzi S, Hillion F, et al. (2008) A single-cell view on the ecophysiology of anaerobic phototrophic bacteria. Proceedings of the National Academy of Sciences 105: 17861-17866.

Nauhaus K, Treude T, Boetius A & Krüger M. (2005) Environmental regulation of the anaerobic oxidation of methane: a comparison of ANME-I and ANME-II communities. Environmental Microbiology 7: 98-106.

Nauhaus K, Albrecht M, Elvert M, Boetius A & Widdel F. (2007) In vitro cell growth of marine archaeal-bacterial consortia during anaerobic oxidation of methane with sulfate. Environmental Microbiology 9: 187-196.

Niemann H, Lösekann T, de Beer D, Elvert M, Nadalig T, Knittel K, et al. (2006) Novel microbial communities of the Haakon Mosby mud volcano and their role as a methane sink. Nature 443: 854-858.

Orphan VJ & House CH. (2009) Geobiological investigations using secondary ion mass spectrometry (SIMS): microanalysis of extant and paleo-microbial processes. Geobiology 7: 360-372. .

Orphan VJ, House CH, Hinrichs K-U, McKeegan KD & DeLong EF. (2002) Multiple archaeal groups mediate methane oxidation in anoxic cold seep sediments. Proceedings of the National Academy of Sciences 99: 7663-7668.

Orphan VJ, House CH, Hinrichs KU, McKeegan KD & DeLong EF. (2001) Methane-consuming archaea revealed by directly coupled isotopic and phylogenetic analysis. Science 293: 484-487.

Orphan VJ, Ussler W, Naehr TH, House CH, Hinrichs KU & Paull CK. (2004) Geological, geochemical, and microbiological heterogeneity of the seafloor around methane vents in the Eel River Basin, offshore California. Chemical Geology 205: 265-289.

Ottesen EA, Hong JW, Quake SR & Leadbetter JR. (2006) Microfluidic digital PCR enables multigene analysis of individual environmental bacteria. Science 314: 1464-1467.

Pace NR, Stahl DA, Lane DJ & Olsen GJ. (1985) Analyzing natural microbial populations by rRNA sequences. ASM American Society for Microbiology News 51: 4-12.

Pernthaler A, Dekas AE, Brown CT, Goffredi SK, Embaye T & Orphan VJ. (2008) Diverse syntrophic partnerships from deep-sea methane vents revealed by direct cell capture and metagenomics. Proc Natl Acad Sci U S A 105: 7052-7057.

Preisler A, de Beer D, Lichtschlag A, Lavik G, Boetius A & Jorgensen BB. (2007) Biological and chemical sulfide oxidation in a Beggiatoa inhabited marine sediment. ISME J 1: 341-353.

Prosser JI. (2012) Ecosystem processes and interactions in a morass of diversity. Fems Microbiology Ecology.

Rabus R, Hansen T & Widdel F. (2006) Dissimilatory sulfate-and sulfur-reducing prokaryotes. The prokaryotes 2: 659-768.

Reeburgh WS. (1976) Methane consumption in Cariaco Trench waters and sediments. Earth and Planetary Science Letters 28: 337-344.

Rossel PE, Elvert M, Ramette A, Boetius A & Hinrichs K-U. (2011) Factors controlling the distribution of anaerobic methanotrophic communities in marine environments: Evidence from intact polar membrane lipids. Geochimica et Cosmochimica Acta 75: 164-184.

Sahling H, Masson DG, Ranero CR, Hühnerbach V, Weinrebe W, Klauke I, et al. (2008) Fluid seepage at the continental margin offshore Costa Rica and southern Nicaragua. Geochemistry Geophysics Geosystems 9: Q05S05.

Sahling H, Rickert D, Lee RW, Linke P & Suess E. (2002) Macrofaunal community structure and sulfide flux at gas hydrate deposits from the Cascadia convergent margin, NE Pacific. Marine Ecology Progress Series 231: 121-138.

Schramm A, Fuchs BM, Nielsen JL, Tonolla M & Stahl DA. (2002) Fluorescence *in situ* hybridization of 16S rRNA gene clones (Clone-FISH) for probe validation and screening of clone libraries. Environmental Microbiology 4: 713-720.

Schreiber L, Holler T, Knittel K, Meyerdierks A & Amann R. (2010) Identification of the dominant sulfate-reducing bacterial partner of anaerobic methanotrophs of the ANME-2 clade. Environmental Microbiology 12: 2327-2340.

Torres ME, McManus J, Hammond DE, de Angelis MA, Heeschen KU, Colbert SL, et al. (2002) Fluid and chemical fluxes in and out of sediments hosting methane hydrate deposits on Hydrate Ridge, OR, I: Hydrological provinces. Earth and Planetary Science Letters 201: 525-540.

Torsvik V, Ovreas L & Thingstad TF. (2002) Prokaryotic diversity--magnitude, dynamics, and controlling factors. Science Signalling 296: 1064.

Turley CM. (1993). Direct estimates of bacterial numbers in seawater samples without incurring cell loss due to sample storage. In Kemp, P.F., Sherr, B.F., Sherr, E.B. and Cole, J.J. (ed.). Handbook of methods in aquatic microbial ecology. Lewis Publishers, Boca Raton, Fla: pp 143-147

Valentine DL & Reeburgh WS. (2000) New perspectives on anaerobic methane oxidation. Environ Microbiol 2: 477-484.

Wagner M, Horn M & Daims H. (2003) Fluorescence *in situ* hybridisation for the identification and characterisation of prokaryotes. Current Opinion in Microbiology 6: 302-309.

FIGURES

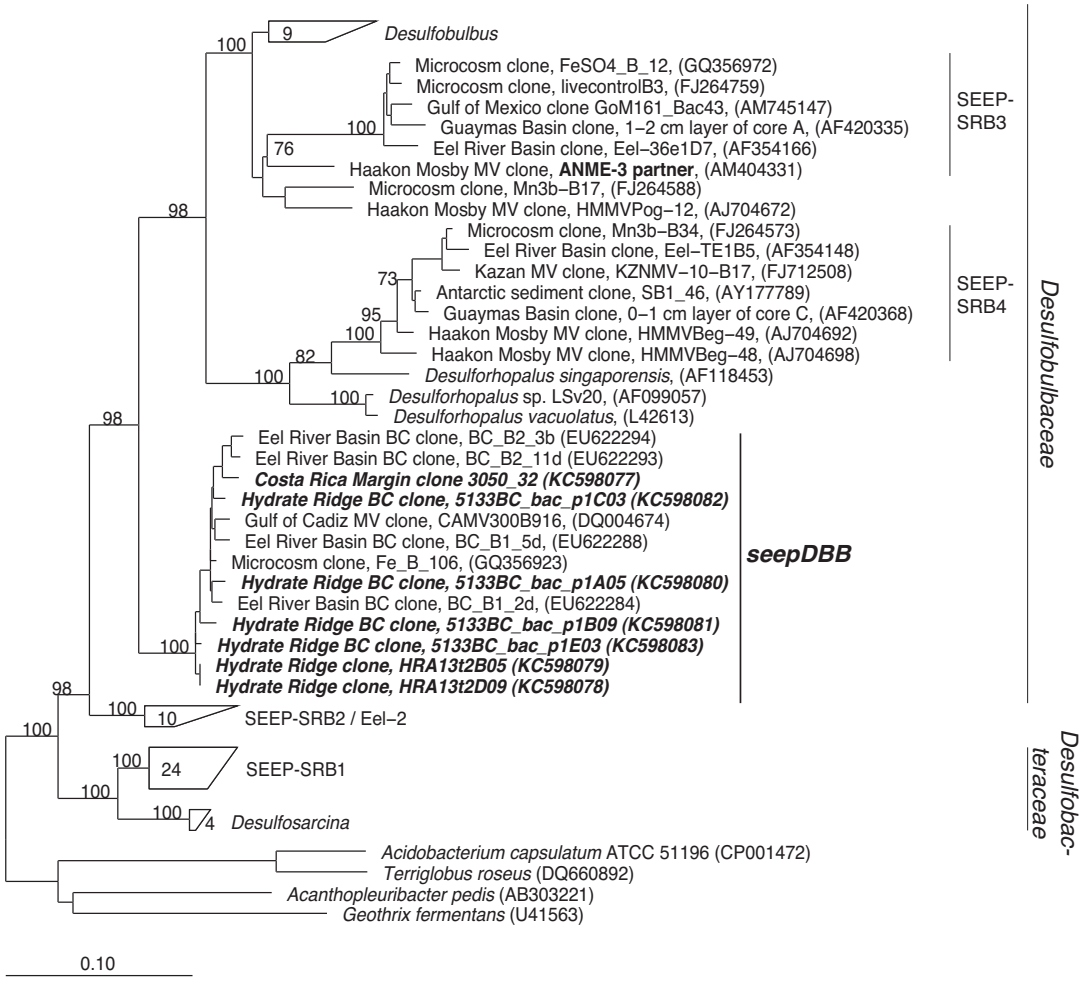

Figure 1

16S rRNA gene phylogeny of pure culture representatives and sulfate-reducing *Deltaproteobacterial* sequences retrieved from methane seeps inferred by Neighbor-joining with the Jukes and Cantor model, was used to estimate distances using the ARB database SSURef-108-SILVA-NR (www.arb-silva.de) and the provided bacterial filter. Bootstrap values were obtained in PAUP* 4.0b10 by Neighbor-joining with 1000 bootstraps. Clones from this study were added to the existing full-length 16S rRNA tree using the quick add maximum parsimony method. Scale bar represents 0.10 substitutions per site. BC = Bead-Captured (i.e., originating from magneto-FISH). Sequences from the current study are in bold italices.

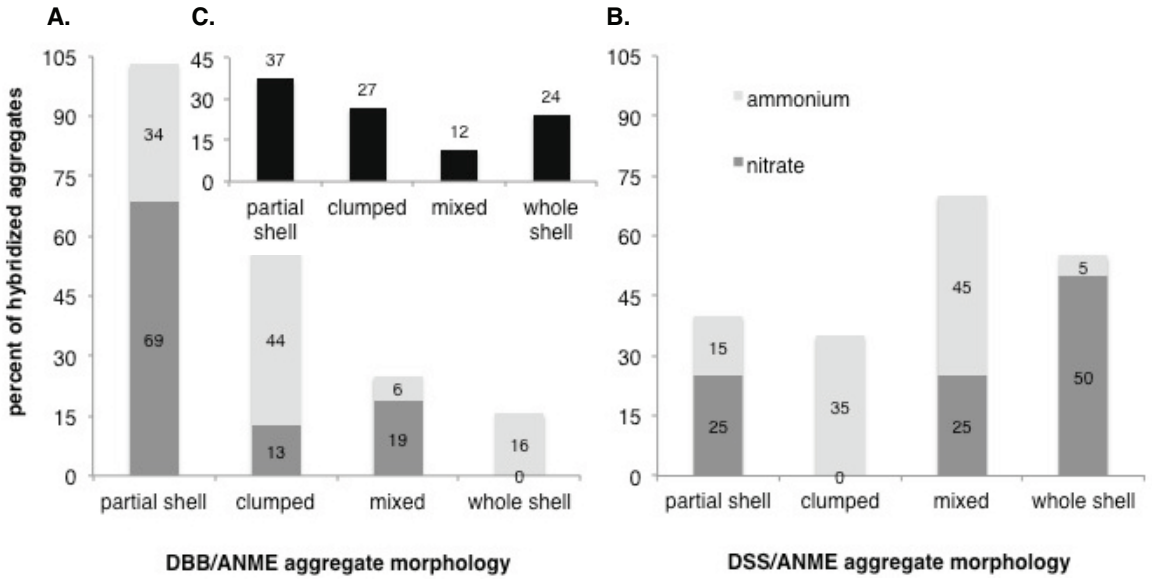

Figure 2
Relative proportions of total aggregate morphologies from (A and B) nitrogen amended incubations or (B) push core sediments collected from Eel River Basin.

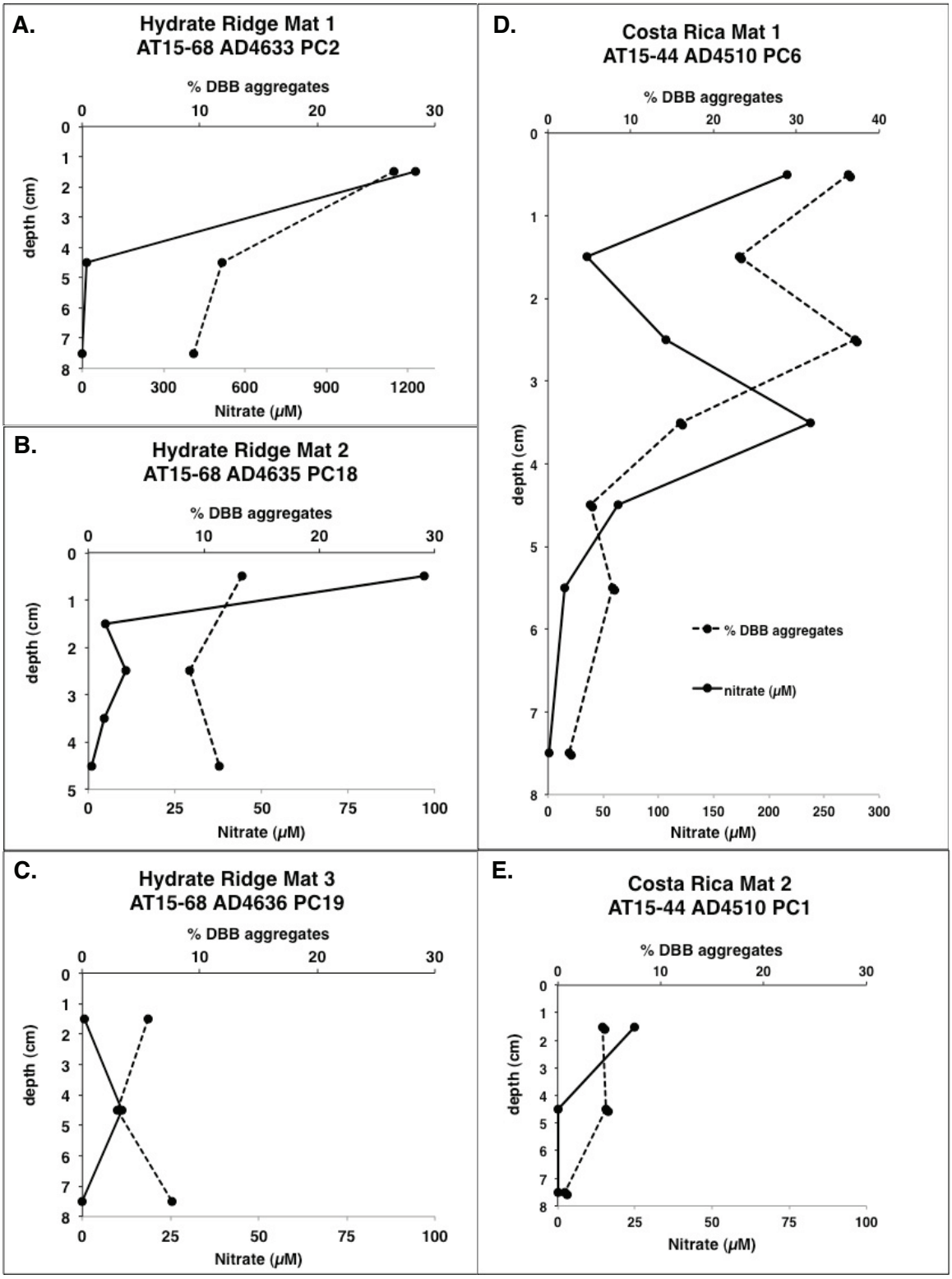
A.
Hydrate Ridge Mat 1
AT15-68 AD4633 PC2
% DBB aggregates
depth (cm)
Nitrate (μM)
B.
Hydrate Ridge Mat 2
AT15-68 AD4635 PC18
% DBB aggregates
depth (cm)
Nitrate (μM)
C.
Hydrate Ridge Mat 3
AT15-68 AD4636 PC19
% DBB aggregates
depth (cm)
Nitrate (μM)
D.
Costa Rica Mat 1
AT15-44 AD4510 PC6
% DBB aggregates
depth (cm)
% DBB aggregates
nitrate (μM)
Nitrate (μM)
E.
Costa Rica Mat 2
AT15-44 AD4510 PC1
% DBB aggregates
depth (cm)
Nitrate (μM)

Figure 3
Nitrate depth profiles and relative abundance of ANME/seepDBB (to total ANME/SRB) aggregate distribution from push cores collected from (A, B and C) Hydrate Ridge and (D and E) Costa Rica Margin methane seep.

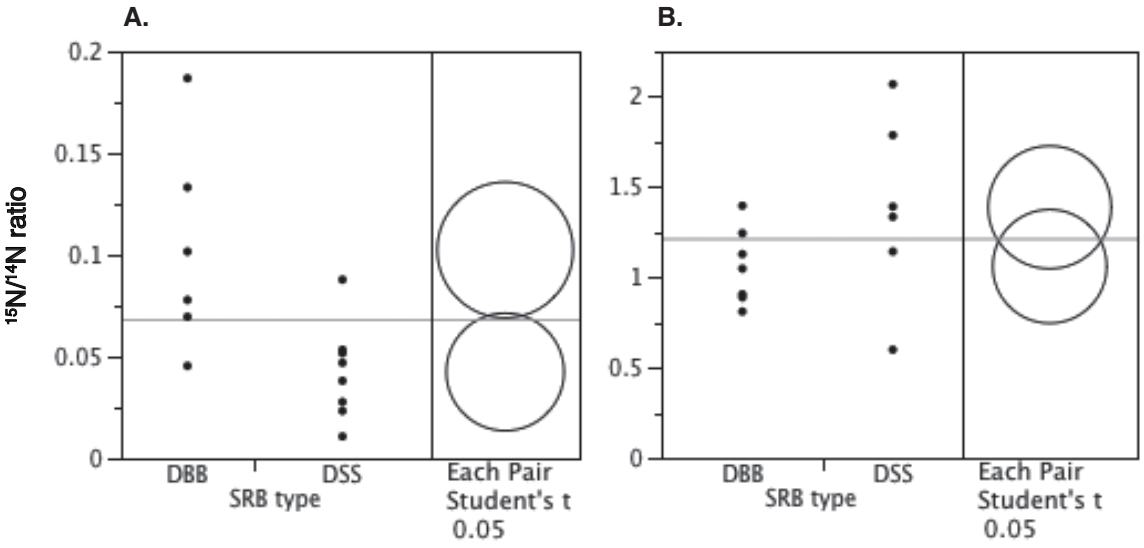

Figure 4
^{15}N enrichment measured via NanoSIMS in ANME/seepDBB and ANME/DSS aggregates from incubations of Eel River Basin methane seep sediment and amended with either (A) ^{15}N-nitrate or (B) ^{15}N-ammonium.

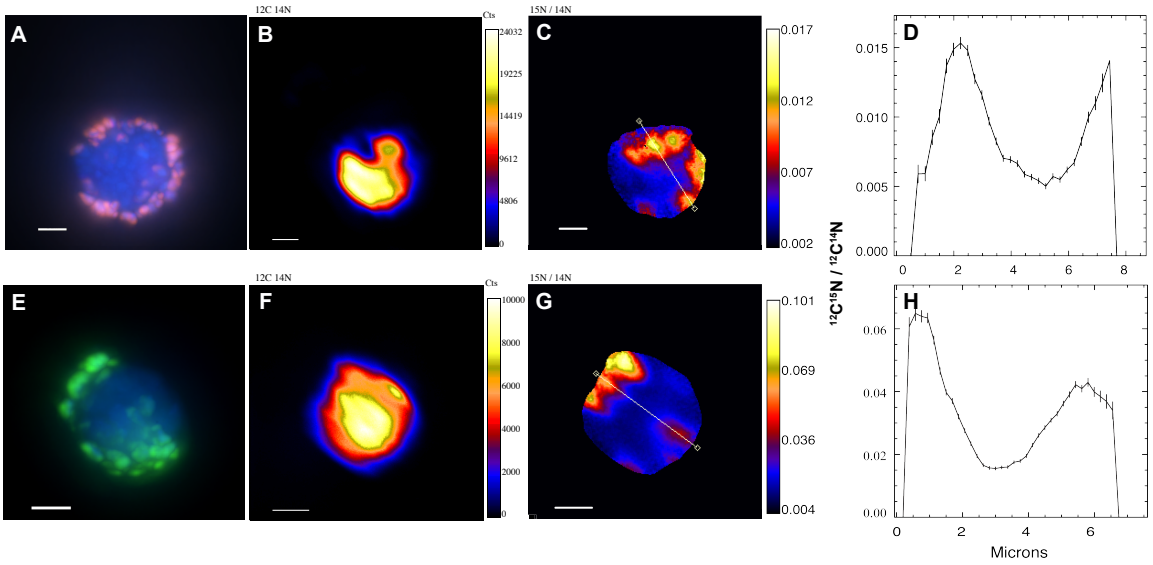

Figure 5

Examples of (A-D) ANME/DSS or (E-H) ANME/seepDBB aggregates from ^{15}N-nitrate incubations that show ^{15}N enrichment in SRB region of aggregate. (B and F) ^{12}C ^{14}N isotope images. (D and H) ^{15}N enrichment profiles of transects through adjacent (C and G) ^{15}N/^{14}N isotope images. Scale bar represents 2 µm.

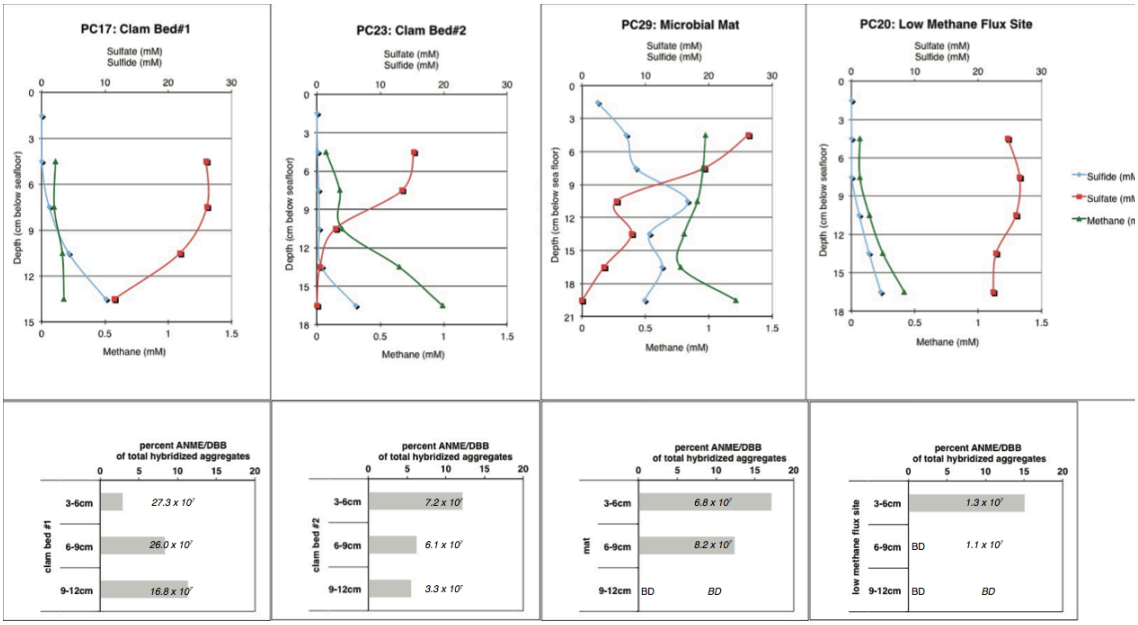

Figure S1

(top panel) Methane, sulfate and sulfide depth profiles and (lower panel) relative abundance of ANME/seepDBB (to total ANME/SRB) aggregate distribution from push cores collected from three habitats along the same transect in Eel River Basin methane seep. (lower panel) Bars represent relative abundance of ANME/seepDBB (to total ANME/SRB); numbers on bars represent total aggregates/ml (as estimated via DAPI counts). BD = below detection.

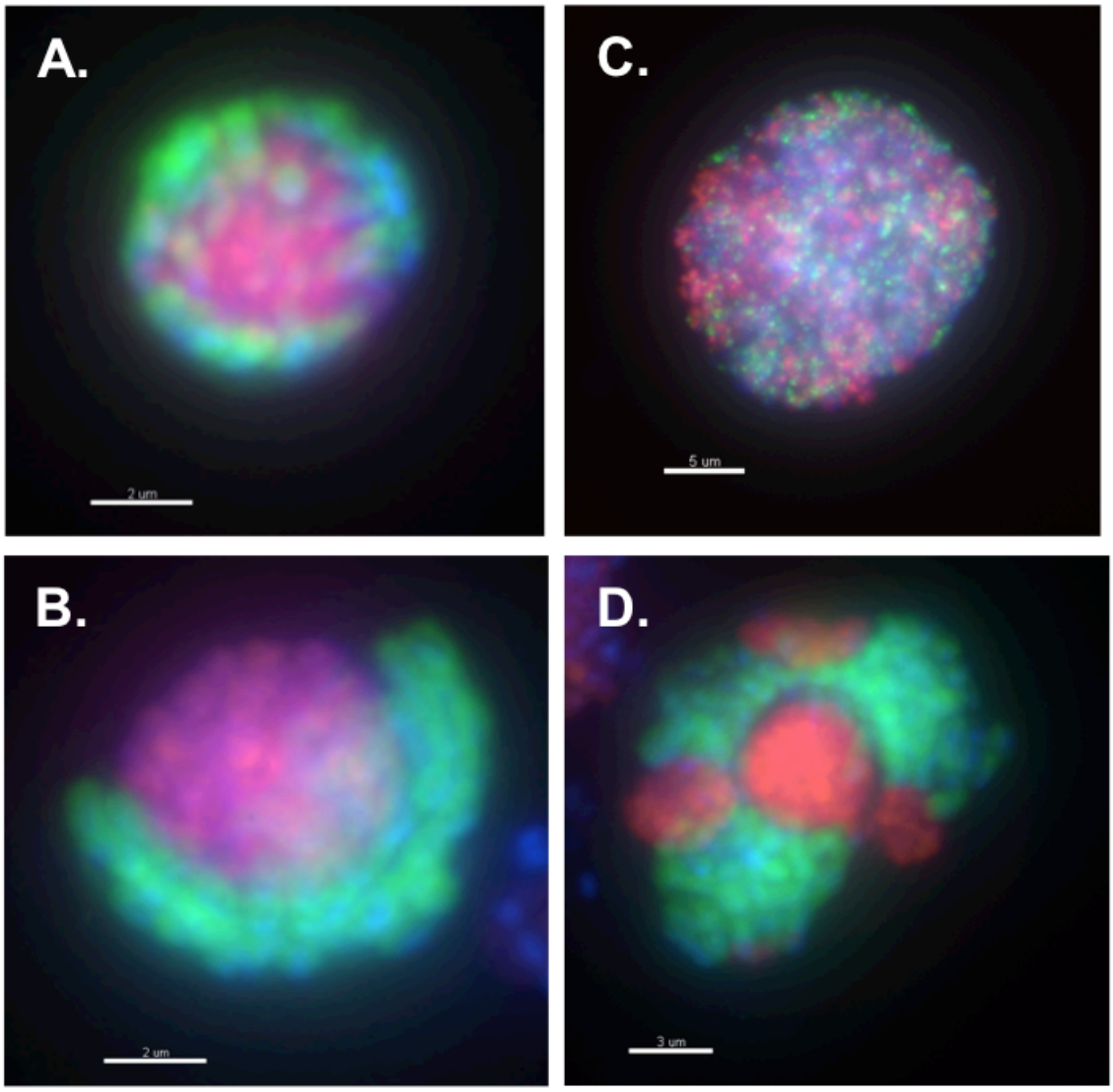

Figure S2
Examples of (A) shell, (B) partial shell, (C) mixed and (D) clumped aggregate morphology. Aggregates were hybridized with probes seepDBB653 (green; targeting methane seep Desulfobulbaceae; this study) and EelMsMX_932 (red; targeting ANME; Boetius et al., 2000). All cells were counter stained (blue) using DAPI.

sample name	location	date	cruise	dive	latitude and longitude	depth (mbsl)	push core	sediment depths (cmbsf)	habitat	sample first described	analysis
	Eel River Basin	**Oct-06**	**AT 15-11**								
clam1	Northern Ridge			AD4256	40°N 48.6 124°W 36.6	520	PC17	3 to 12	clam bed	this study	agg. counts, geochemistry
low-methane	Northern Ridge			AD4256	40°N 48.6 124°W 36.6	520	PC20	3 to 12	low methane	this study	agg. counts, geochemistry
clam2	Northern Ridge			AD4256	40°N 48.6 124°W 36.6	520	PC23	3 to 12	clam bed	this study	agg. counts, geochemistry
mat	Northern Ridge			AD4256	40°N 48.6 124°W 36.6	520	PC29	3 to 12	microbial mat	Pernthaler et al., 2008	DNA, agg. counts, geochemistry
incubation, PC11	Southern Ridge			AD4254	40°N 47.2 124°W 35.7	520	PC11	0 to 12	clam bed	Dekas et al., 2009	FISH-nanoSIMS, agg. counts
incubation, PC14	Southern Ridge			AD4254	40°N 47.2 124°W 35.7	520	PC14	0 to 15	microbial mat	Dekas et al., 2009	FISH-nanoSIMS
	Costa Rica Margin	**Feb-09**	**AT 15-44**								
Costa Rica Mat 1	Jaco Summit			AD4510	9°N 10.3 84°W 47.9	745	PC6	0 to 9	microbial mat	Dekas et al., in review	DNA, agg. counts, geochemistry
Costa Rica Mat 2	Jaco Summit			AD4510	9°N 10.3 84°W 47.9	745	PC1	0 to 9	microbial mat	Dekas et al., in review	agg. counts, geochemistry
	Hydrate Ridge	**Aug-10**	**AT 15-68**								
Hydrate Ridge Mat 1	Southeast Knoll			AD4633	44°N 27.0 125°W 1.7	625	PC2	0 to 9	microbial mat	this study	agg. counts, geochemistry
Hydrate Ridge Mat 2	Hydrate Ridge South			AD4635	44°N 34.1 125°W 9.1	775	PC18	0 to 6	microbial mat	this study	agg. counts, geochemistry
Hydrate Ridge Mat 3	Hydrate Ridge South			AD4636	44°N 34.1 125°W 9.1	772	PC19	0 to 9	microbial mat	this study	agg. counts, geochemistry
DNA sample	Hydrate Ridge South			AD4629	44°N 34.1 125°W 9.1	774	PC9	0 to 3	microbial mat	this study	DNA
	Hydrate Ridge	**Sep-11**	**AT 18-10**								
DNA sample	Hydrate Ridge North			J2 593 E3	44°N 40.0 125°W 6.0	600	PC47	0 to 9	microbial mat	this study	DNA

Table S1. Summary of samples used in this study. mbsl = meters below sea level, cmbsf = centimeters below sea floor, agg = aggregate